



This is a repository copy of *RAFT dispersion polymerization in non-polar solvents: facile production of block copolymer spheres, worms and vesicles in n-alkanes*.

White Rose Research Online URL for this paper:  
<http://eprints.whiterose.ac.uk/78465/>

---

**Article:**

Fielding, L.A., Derry, M.J., Ladmiraal, V. et al. (5 more authors) (2013) RAFT dispersion polymerization in non-polar solvents: facile production of block copolymer spheres, worms and vesicles in n-alkanes. *Chemical Science*, 4 (5). 2081 - 2087. ISSN 2041-6520

<https://doi.org/10.1039/c3sc50305d>

---

**Reuse**

Items deposited in White Rose Research Online are protected by copyright, with all rights reserved unless indicated otherwise. They may be downloaded and/or printed for private study, or other acts as permitted by national copyright laws. The publisher or other rights holders may allow further reproduction and re-use of the full text version. This is indicated by the licence information on the White Rose Research Online record for the item.

**Takedown**

If you consider content in White Rose Research Online to be in breach of UK law, please notify us by emailing [eprints@whiterose.ac.uk](mailto:eprints@whiterose.ac.uk) including the URL of the record and the reason for the withdrawal request.



[eprints@whiterose.ac.uk](mailto:eprints@whiterose.ac.uk)  
<https://eprints.whiterose.ac.uk/>

*promoting access to White Rose research papers*



**Universities of Leeds, Sheffield and York**  
**<http://eprints.whiterose.ac.uk/>**

---

This is an author produced version of a paper published in **Chemical Science**.

White Rose Research Online URL for this paper:

<http://eprints.whiterose.ac.uk/78465>

---

**Published paper**

Fielding, L.A., Derry, M.J., Ladmiral, V., Rosselgong, J., Rodrigues, A.M., Ratcliffe, L.P.D., Sugihara, S. and Armes, S.P. (2013) *RAFT dispersion polymerization in non-polar solvents: facile production of block copolymer spheres, worms and vesicles in n-alkanes*. *Chemical Science*, 4 (5). 2081 - 2087.  
ISSN 2041-6520

<http://dx.doi.org/10.1039/c3sc50305d>

---

*White Rose Research Online*  
*[eprints@whiterose.ac.uk](mailto:eprints@whiterose.ac.uk)*

---

# RAFT Dispersion Polymerization in Non-Polar Solvents: Facile Production of Block Copolymer Spheres, Worms and Vesicles in *n*-Alkanes

Lee A. Fielding<sup>\*a</sup>, Matthew J. Derry<sup>a</sup>, Vincent Ladmiral<sup>b</sup>, Julien Rosselgong<sup>c</sup>, Aurélie M. Rodrigues<sup>d</sup>,  
Liam P. D. Ratcliffe<sup>a</sup>, Shinji Sugihara<sup>e</sup> and Steven P. Armes<sup>\*a</sup>

**ABSTRACT.** Well-defined poly(lauryl methacrylate-benzyl methacrylate) (PLMA-PBzMA) diblock copolymer nanoparticles are prepared in *n*-heptane at 90°C via reversible addition-fragmentation chain transfer (RAFT) polymerization. Under these conditions, the PLMA macromolecular chain transfer agent (macro-CTA) is soluble in *n*-heptane, whereas the growing PBzMA block quickly becomes insoluble.

Thus this dispersion polymerization formulation leads to polymerization-induced self-assembly (PISA). Using a relatively long PLMA macro-CTA with a mean degree of polymerization (DP) of 37 or higher leads to the formation of well-defined spherical nanoparticles of 41 to 139 nm diameter, depending on the DP targeted for the PBzMA block. In contrast, TEM studies confirm that using a relatively short PLMA macro-CTA (DP = 17) enables both worm-like and vesicular morphologies to be produced, in addition to the spherical phase. A detailed phase diagram has been elucidated for this more asymmetric diblock copolymer formulation, which ensures that each phase can be targeted reproducibly. <sup>1</sup>H NMR spectroscopy confirmed that high BzMA monomer conversions (> 97 %) were achieved within 5 h, while GPC studies indicated that reasonably good blocking efficiencies and relatively low diblock copolymer polydispersities ( $M_w/M_n < 1.30$ ) were obtained in most cases. Compared to prior literature reports, this all-methacrylic PISA formulation is particularly novel because: (i) it is the first time that higher order morphologies (e.g. worms and vesicles) have been accessed in non-polar solvents and (ii) such diblock copolymer nano-objects are particularly relevant to potential boundary lubrication applications for engine oils.

## Introduction

Currently, there is strong academic interest in polymerization-induced self-assembly (PISA)<sup>1-3</sup> using living radical polymerization techniques such as reversible addition-fragmentation chain transfer (RAFT) polymerization.<sup>4-8</sup> This approach has enormous potential for the design of bespoke organic ‘nano-objects’ of controlled size and morphology without any further processing steps. For example, RAFT aqueous dispersion polymerization has been utilized to grow a water-insoluble core-forming block from a water-soluble stabilizer block in order to prepare a range of sterically-stabilized diblock copolymer nanoparticles.<sup>9-14</sup> Spherical morphologies are most commonly obtained,<sup>9-13</sup> but systematic variation of the block copolymer composition coupled with a detailed knowledge of the block copolymer phase diagram also allows access to higher order morphologies such as worms<sup>14-16</sup> and vesicles.<sup>17-26</sup> In most cases good blocking efficiencies and reasonably low final polydispersities (e.g.  $M_w/M_n < 1.20$ ) can be achieved, along with very high monomer conversions within relatively short reaction times (e.g. > 99 % after 2 h at 70°C). Given that these diblock copolymer nanoparticles can be prepared directly in water at relatively low solution viscosities at up to 25 % solids, such robust surfactant-free formulations appear to offer real potential for various commercial applications, including readily sterilizable

gels<sup>15</sup> new vectors for intracellular delivery<sup>27</sup> and novel Pickering emulsifiers.<sup>28</sup>

Similarly, RAFT dispersion polymerization in polar solvents such as lower alcohols has been extensively explored by Pan et al.,<sup>29-34</sup> by Charleux and co-workers,<sup>35, 36</sup> and also by our own research group.<sup>25, 26</sup> Again, pure spherical, worm-like and vesicular morphologies have all been observed, depending on the targeted diblock composition. GPC analyses confirm that fairly good control over the copolymer molecular weight distribution (e.g.  $M_w/M_n < 1.20-1.30$ ) can be achieved for such heterogeneous formulations, as expected for well-behaved RAFT syntheses. Substantially incomplete monomer conversions were reported by Pan et al.,<sup>29-34</sup> but this technical problem can be solved by switching to an all-methacrylic formulation in which the core-forming styrene monomer is replaced with benzyl methacrylate.<sup>25, 26, 35</sup>

Despite the current intense activity in PISA syntheses, there are remarkably few literature reports of RAFT dispersion polymerization being attempted in *low polarity* solvents.<sup>37-39</sup> Moreover, significant technical problems have been encountered to date. For example, Ji et al. were unable to obtain monomer conversions greater than around 50 % for the alternating copolymerization of styrene and maleic anhydride conducted in chloroform using a poly(ethylene oxide)-based RAFT agent because one of the comonomers (maleic anhydride) was excluded

from the growing copolymer micelle cores.<sup>37</sup> Charleux and co-workers reported an all-acrylic RAFT dispersion polymerization formulation conducted in isododecane based on a poly(2-ethylhexyl acrylate) macro-CTA and a poly(methyl acrylate) core-forming block.<sup>38</sup> Near-monodisperse spherical nanoparticles ranging from 30 to 54 nm (as judged by DLS) could be prepared using a trithiocarbonate-based macro-CTA, whereas a dithiobenzoate-based macro-CTA suffered from strong rate retardation and relatively poor control. However, it is emphasized that only spherical morphologies were obtained in this prior study. Moreover, no electron microscopy studies were undertaken, presumably because of the film-forming nature of the core-forming poly(methyl acrylate) block.

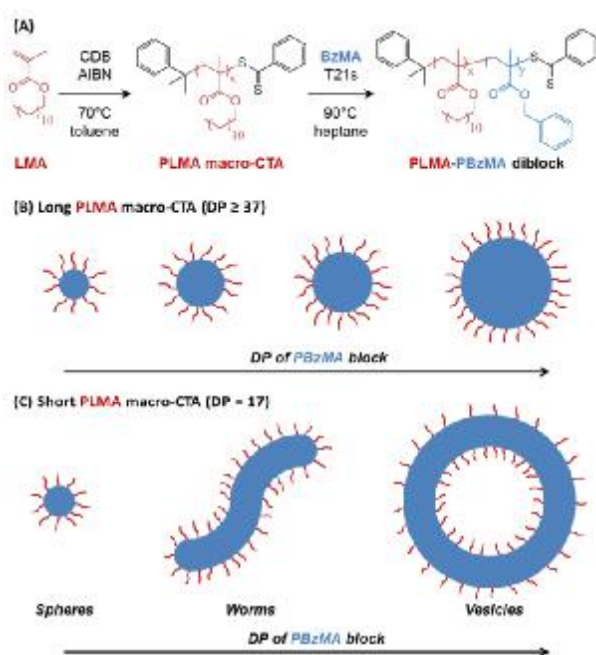


**Fig. 1** (A) RAFT synthesis of poly(lauryl methacrylate) (PLMA) macro-CTA via solution polymerization in toluene at 70°C followed by RAFT dispersion polymerization of benzyl methacrylate (BzMA) in *n*-heptane at 90°C. (B) Schematic representation of the change in size that can occur on increasing the PBzMA target degree of polymerization when using a relatively long PLMA macro-CTA (DP ≥ 37). (C) Schematic representation of the change in morphology that can occur on increasing the PBzMA target degree of polymerization when using a relatively short PLMA macro-CTA (DP = 17).

From a purely scientific perspective, a successful RAFT dispersion polymerization formulation would serve to emphasize the universal applicability of the PISA approach for the design of bespoke diblock copolymer nanoparticles. Moreover, in the light of recent work by Liu and co-workers<sup>40</sup> there is the genuine prospect that such nanoparticles might prove to be highly effective cost-effective boundary lubricants for engine oils. In principle, this could enable significant improvements to be made in terms of fuel economy, while at the same time reducing automotive emissions and hence enhancing air quality.

Herein, we describe the first all-methacrylic *n*-alkane-based RAFT dispersion polymerization formulation: a poly(lauryl methacrylate)-based macro-CTA is extended using benzyl methacrylate to produce diblock copolymer nanoparticles in *n*-

heptane at 90°C (Figure 1A). For relatively long macro-CTAs, systematic variation of the target degree of polymerization (DP) of the core-forming poly(benzyl methacrylate) block allows a range of well-defined spherical nanoparticles of tuneable particle size to be produced (Figure 1B). Moreover, we report the first observation of higher order morphologies prepared via RAFT dispersion polymerization in *n*-alkanes. More specifically, the judicious selection of a relatively short macro-CTA enables both worm-like and vesicular morphologies to be obtained (Figure 1C). Thus the same morphological control previously reported for aqueous and alcoholic formulations can also be achieved for RAFT polymerizations conducted in non-polar solvents, which further demonstrates the universal applicability of such PISA formulations.

## Experimental

### Materials

Monomers were purchased from Sigma-Aldrich (UK) and passed through basic alumina prior to use. Tert-butyl peroxy-2-ethylhexanoate (Trigonox 21S or T21s) initiator was supplied by Akzo Nobel (The Netherlands). All other reagents were purchased from Sigma-Aldrich (UK) and were used as received, unless otherwise noted. Tetrahydrofuran (THF) and *n*-heptane were purchased from Fisher Scientific (UK), and deuterated methylene chloride (CD<sub>2</sub>Cl<sub>2</sub>) was purchased from Goss Scientific (UK). 4-cyano-4-((2-phenylethanesulfanyl)thiocarbonyl)sulfanyl)pentanoic acid (PETTC) was prepared in-house and the synthesis has been described in detail elsewhere.<sup>21</sup>

### Synthesis of poly(lauryl methacrylate) macro-chain transfer agent

A typical synthesis of PLMA<sub>17</sub> macro-CTA was conducted as follows. A round-bottomed flask was charged with LMA (20.0 g; 78.6 mmol), cumyl dithiobenzoate (CDB; 2.142 g; 7.86 mmol), 2,2'-azobisisobutyronitrile (AIBN; 258 mg, 1.57 mmol; CDB/AIBN molar ratio = 5.0) and toluene (33.0 g). The sealed reaction vessel was purged with nitrogen and placed in a pre-heated oil bath at 70°C for 11 h. The resulting PLMA (LMA conversion = 85 %;  $M_n = 4\,900\text{ g mol}^{-1}$ ,  $M_w = 5\,900\text{ g mol}^{-1}$ ,  $M_w/M_n = 1.20$ ) was purified by precipitation into excess methanol. The mean degree of polymerization (DP) of this macro-CTA was calculated to be 17 using <sup>1</sup>H NMR by comparing the integrated signals corresponding to the CDB aromatic protons at 7.1-8.1 ppm with that assigned to the two oxymethylene protons due to PLMA at 3.7-4.2 ppm. Further PLMA macro-CTAs with higher mean target DPs (up to 70; see Supporting Information, Table S1) were synthesized using either CDB, PETTC or 2-cyano-2-propyl dithiobenzoate (CPDB) using similar conditions and were purified by precipitation into excess methanol or acetone.

### Synthesis of poly(lauryl methacrylate)-poly(benzyl methacrylate) (PLMA-PBzMA) diblock copolymer particles

A typical RAFT dispersion polymerization synthesis of PLMA<sub>17</sub>-PBzMA<sub>300</sub> at 15 w/w % solids was conducted as follows. BzMA (1.15 g; 6.53 mmol), T21s initiator (2.35 mg; 0.011 mmol) and PLMA<sub>17</sub> macro-CTA (0.10 g; 0.022 mmol; macro-CTA/initiator

molar ratio = 2.0) were dissolved in *n*-heptane (7.08 g). The reaction mixture was sealed in a round-bottomed flask and purged with nitrogen gas for 25 min while immersed in an ice bath so as to reduce solvent evaporation. The deoxygenated solution was then placed in a pre-heated oil bath at 90°C for 24 h (final BzMA conversion = 98 %;  $M_n = 57\,100\text{ g mol}^{-1}$ ,  $M_w = 67\,600\text{ g mol}^{-1}$ ,  $M_w/M_n = 1.18$ ). In further syntheses, the mean DP of the PBzMA block was systematically varied by adjusting the amount of added BzMA monomer. Some syntheses were also performed at a higher macro-CTA/initiator ratio of 5.0, which is known to provide better control over the molecular weight distribution (albeit at the expense of a slower rate of polymerization).<sup>5, 41, 42</sup>

### Gel permeation chromatography

Molecular weight distributions were assessed by gel permeation chromatography (GPC) using THF eluent. The THF GPC system was equipped with two 5  $\mu\text{m}$  (30 cm) Mixed C columns; a WellChrom K-2301 refractive index detector operating at 950  $\pm$  30 nm, a Precision detector PD 2020 light scattering detector (with scattering angles of 90° and 15°), and a BV400RT solution viscosity detector. The THF mobile phase contained 2 v/v % triethylamine and 0.05 w/v % butylhydroxytoluene (BHT) and the flow rate was fixed at 1.0 mL min<sup>-1</sup>. A series of ten near-monodisperse poly(methyl methacrylate) standards ( $M_p$  values ranging from 1,280 to 330,000 g mol<sup>-1</sup>) were used for calibration.

### <sup>1</sup>H NMR spectroscopy

<sup>1</sup>H NMR spectra were recorded in either CD<sub>2</sub>Cl<sub>2</sub> or CDCl<sub>3</sub> using a Bruker AV1-400 or AV1-250 MHz spectrometer. Typically sixty four scans were averaged per spectrum.

### Dynamic light scattering

Dynamic light scattering (DLS) studies were performed using a Zetasizer Nano-ZS instrument (Malvern Instruments, UK) at 25°C at a scattering angle of 173°. Copolymer dispersions were diluted in *n*-heptane prior to light scattering studies. The intensity-average diameter and polydispersity (PDI) of the diblock copolymer particles were calculated by cumulants analysis of the experimental correlation function using Dispersion Technology Software version 6.20. Data were averaged over thirteen runs each of thirty seconds duration. It should be noted that DLS reports intensity-average diameters and implicitly assumes a spherical morphology. Thus the DLS dimensions reported for anisotropic worm-like particles herein are actually sphere-equivalent diameters that do not provide accurate information regarding either the worm length or the worm width. Nevertheless, DLS observations of a significantly larger particle size (and also greater polydispersity) are a useful indication of the presence of worm-like morphologies as either a pure or as one or more mixed phases.

### Transmission electron microscopy

Transmission electron microscopy (TEM) studies were conducted using a Philips CM 100 instrument operating at 100 kV and equipped with a Gatan 1 k CCD camera. Diluted block copolymer solutions (0.5 w/w %) were placed on carbon-coated copper grids and exposed to ruthenium(IV) oxide vapor for 7 minutes at 20°C prior to analysis.<sup>43</sup> This heavy metal compound

acted as a positive stain to improve contrast. The ruthenium(IV) oxide was prepared as follows: ruthenium(II) oxide (0.30 g) was added to water (50 g) to form a black slurry; addition of sodium periodate (2.0 g) with stirring produced a yellow solution of ruthenium(IV) oxide within 1 min.

## Results and Discussion

There are at least two reports of the synthesis of spherical nanoparticles in *n*-alkanes using either so-called ‘group transfer’ polymerization of methyl methacrylate<sup>44</sup> or the classical anionic polymerization of styrene<sup>45</sup> under dispersion polymerization conditions. However, such living polymerization formulations involved the use of pre-formed polystyrene-based diblock copolymer micelles to prevent macroscopic precipitation of the growing polymer chains, rather than chain extension of a soluble stabilizer block by an insoluble block (as in the present study).

Both our group<sup>15, 17-26</sup> and other workers<sup>9-13, 29-36</sup> have reported that chain extension of a RAFT macro-CTA under dispersion polymerization conditions leads to the formation of a range of diblock copolymer nano-objects in either aqueous or alcoholic media. In the present study, we demonstrate the versatility and broad applicability of this approach by extending such PISA formulations to include non-polar media (e.g. *n*-heptane). This is achieved by chain-extending a poly(lauryl methacrylate) (PLMA) macro-CTA using benzyl methacrylate (BzMA). The latter monomer was chosen because the growing PBzMA block is insoluble in *n*-heptane, which drives *in situ* self-assembly to form diblock copolymer spheres, worms or vesicles depending on the precise reaction conditions.

### PLMA macro-CTA synthesis

RAFT solution polymerization of LMA was conducted in toluene at 70°C to produce a range of low polydispersity PLMA macro-CTAs with varying mean degrees of polymerization. PLMA macro-CTAs were readily prepared using either dithiobenzoate- or trithiocarbonate-based CTAs and in all cases LMA polymerizations were terminated at 73-95 % conversion in order to ensure retention of end-group fidelity. Table S1 summarizes the various PLMA macro-CTAs used in this study: all entries have relatively narrow molecular weight distributions ( $M_w/M_n < 1.26$ ), as expected for well-controlled RAFT syntheses.<sup>4</sup> Figure S1 shows typical kinetic data obtained during the RAFT polymerization of LMA in toluene at 70°C using CPDB. Relatively high conversions (75 %) are attained within 5 h and the linear semi-logarithmic plot indicates first-order kinetics with respect to monomer. The linear evolution in molecular weight with conversion indicates pseudo-living behaviour: this is consistent with GPC studies, which confirm that polydispersities remain below 1.15 throughout the polymerization. A <sup>1</sup>H NMR spectrum of a PLMA<sub>17</sub> macro-CTA is shown in Figure S2 and the corresponding GPC curve is shown in Figure 2B. Comparing the integrated aromatic signals assigned to the CTA end-group at 7.1 to 8.1 ppm to that of the oxymethylene protons due to the LMA repeat units at 3.7 to 4.2 ppm allows the mean degree of polymerization of the macro-CTA to be calculated.

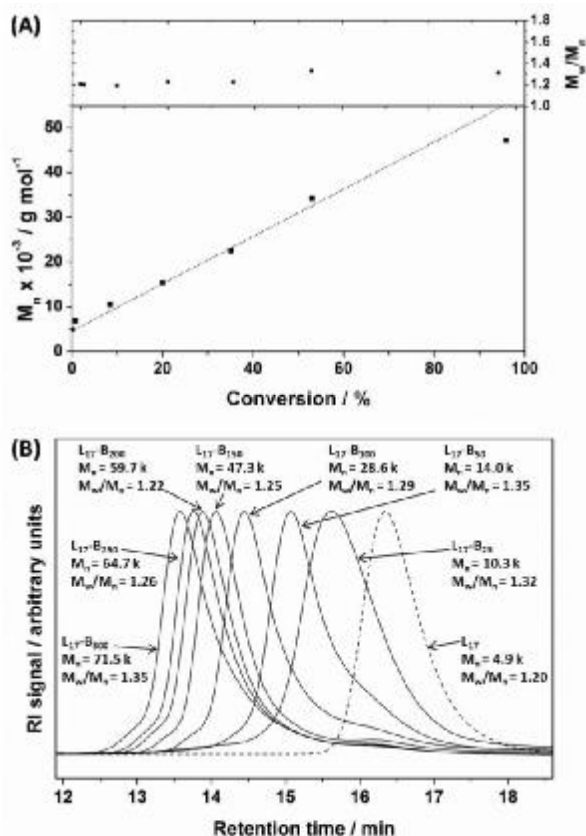


**Fig.2** (A) Evolution of the number-average molecular weight ( $M_n$ ) and polydispersity ( $M_w/M_n$ ) with monomer conversion as judged by THF GPC when using a PLMA<sub>17</sub> macro-CTA for the RAFT dispersion polymerization of BzMA in *n*-heptane at 90 °C and 15 wt. % solids. The targeted diblock composition was PLMA<sub>17</sub>-PBzMA<sub>300</sub> and the PLMA macro-CTA/initiator molar ratio was 2.0. The theoretical dashed straight line assumes perfect macro-CTA blocking efficiency and that no GPC calibration error is incurred when using PMMA standards to analyze these methacrylic diblock copolymers. The non-zero y-intercept indicates the PMMA-equivalent GPC molecular weight of the PLMA<sub>17</sub> macro-CTA. (B) THF gel permeation chromatograms (vs. poly(methyl methacrylate) standards) obtained for a series of six PLMA<sub>17</sub>-PBzMA<sub>x</sub> diblock copolymers (herein abbreviated to L<sub>17</sub>-B<sub>x</sub> for clarity; see entries 24-28, 31 and 33 in Table S2) synthesized via RAFT dispersion polymerization in *n*-heptane at 90 °C and 20 w/v % solids. The corresponding PLMA<sub>17</sub> macro-CTA (prepared in toluene at 70 °C) is also shown as a reference.

## 20 Diblock copolymer nanoparticles

### Kinetics of RAFT dispersion polymerization of benzyl methacrylate

PLMA macro-CTAs were chain-extended using BzMA under RAFT dispersion polymerization conditions in *n*-heptane at 90°C. Monomer conversion data obtained by <sup>1</sup>H NMR studies are shown in Figure S3 for a target diblock composition of PLMA<sub>17</sub>-PBzMA<sub>300</sub> using T21s initiator and a macro-CTA/initiator molar ratio of 2.0 at 15 % solids (entry 9 in Table S2). The initially homogeneous polymerizing solution becomes translucent after approximately 1 h, as judged by visual inspection. This indicates the onset of micellar nucleation, which immediately leads to partitioning of the BzMA monomer into the growing micelles

from the continuous phase. This higher local monomer concentration results in a significant rate enhancement (see Figure S3), as reported for other RAFT dispersion polymerization formulations.<sup>20, 21, 26</sup> A BzMA monomer conversion of 95 % is attained after around 5 h, which indicates that the rate of polymerization of this monomer is rather faster than that achieved under RAFT *alcoholic* dispersion conditions.<sup>21, 26</sup> However, this difference is most likely simply due to the higher reaction temperature and the lower macro-CTA/initiator ratio used in the present work.

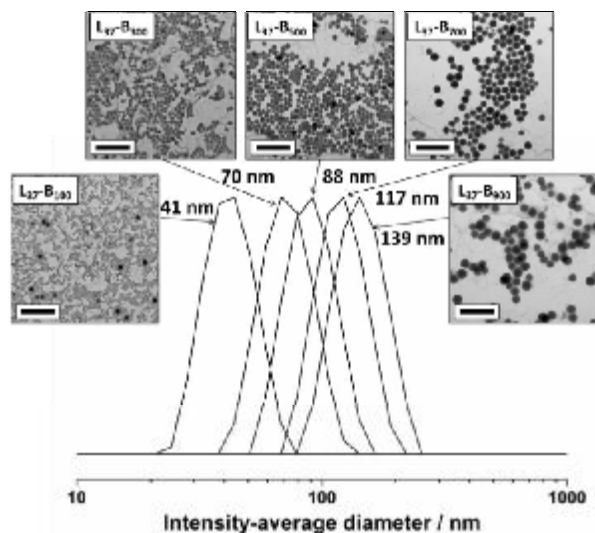


**Fig. 3** Dynamic light scattering particle size distributions obtained for a series of PLMA<sub>37</sub>-PBzMA<sub>x</sub> (herein abbreviated to L<sub>37</sub>-B<sub>x</sub> for clarity; entries 1-5 in Table S4) nanoparticles prepared by RAFT dispersion polymerization of BzMA in *n*-heptane at 90 °C conducted at 15 wt. % solids. Representative TEM images obtained for each of the PLMA<sub>37</sub>-PBzMA<sub>x</sub> compositions are also shown. The scale bar on each image corresponds to 500 nm. The mean diameter of these spherical diblock copolymer nanoparticles can be systematically increased simply by targeting a higher degree of polymerization (*x*) for the core-forming PBzMA block.

The evolution of molecular weight and polydispersity with BzMA monomer conversion is shown in Figure 2A for the same target diblock composition of PLMA<sub>17</sub>-PBzMA<sub>300</sub> using T21s initiator (macro-CTA/initiator molar ratio = 2.0) at 15 % solids (see entry 9 in Table S2). The molecular weight increases linearly with conversion and polydispersities remain below 1.30 throughout the polymerization, as expected for a well-controlled RAFT synthesis. GPC curves obtained for several PLMA<sub>17</sub>-PBzMA<sub>x</sub> diblock copolymers obtained at high conversion are shown in Figure 2B. In most cases relatively high macro-CTA blocking efficiencies are obtained, although there is also some evidence for a low molecular weight shoulder corresponding to unreacted PLMA macro-CTA (or prematurely terminated PLMA<sub>17</sub>-PBzMA<sub>x</sub> chains). However, the refractive index for the PBzMA block is higher than that of the PLMA, hence the apparent level of macro-CTA contamination may be underestimated. The weak high molecular weight shoulder most likely indicates some degree of termination by combination, which probably become more prevalent at high conversions (i.e.

monomer-starved conditions). A macro-CTA/initiator ratio of 2.0 was used in most syntheses as it was found that using a macro-CTA/initiator ratio of 5.0 only resulted in marginally lower polydispersities, but at the expense of longer reaction times (see Table S3). An assigned  $^1\text{H}$  NMR spectrum recorded for a PLMA<sub>17</sub>-PBzMA<sub>50</sub> diblock copolymer (entry 16 in Table S2) obtained at 97 % BzMA conversion is shown in Figure S2.

### Spherical diblock copolymer nanoparticles

Only spherical nanoparticles were obtained in most cases, regardless of the target DP of the PBzMA block (see Table S4). For example, Figure 3 shows typical TEM images obtained for PLMA<sub>37</sub>-PBzMA<sub>x</sub> diblock copolymers synthesized at 15 % solids in *n*-heptane at 90 °C. DLS studies indicate that the intensity-average particle diameter of these nanoparticles can be systematically increased by targeting higher DP values for the core-forming PBzMA block. TEM studies of these PLMA<sub>37</sub>-PBzMA<sub>x</sub> diblock copolymers are consistent with these DLS measurements. In most cases the particle size distributions are relatively narrow. Similar results have been reported for RAFT dispersion polymerizations conducted in either aqueous or alcoholic media.<sup>17, 18, 21, 26</sup>

### Higher order diblock copolymer morphologies

Higher order morphologies could also be obtained for this *n*-alkane RAFT formulation, but only by using a PLMA macro-CTA with a relatively low mean DP of 17. Thus, for a series of PLMA<sub>17</sub>-PBzMA<sub>x</sub> diblock copolymers, a full phase diagram was constructed by systematic variation of (i) the target DP of the core-forming PBzMA block and (ii) the total solids concentration at which the RAFT dispersion polymerization was conducted (see Figure 4A and Table S2). For example, working at 15 % solids and targeting a PBzMA DP of no more than 38 merely produced spherical morphologies. However, targeting a DP of 100 or greater produced polydisperse vesicles as judged by TEM studies, with intermediate target DPs leading to mixed phases.

TEM images obtained for a series of PLMA<sub>17</sub>-PBzMA<sub>x</sub> syntheses conducted at 20 % solids are shown in Figure 4B. Three distinct diblock copolymer morphologies can be clearly observed in this case. Near-monodisperse spheres with a mean diameter of approximately 25 nm are produced when targeting PLMA<sub>17</sub>-PBzMA<sub>25</sub>, whereas anisotropic worms are formed within a relatively narrow compositional range (e.g. PLMA<sub>17</sub>-PBzMA<sub>63</sub>). This very narrow worm phase only corresponds to compositions which produce free-standing gels (as judged by the tube inversion test). Furthermore, it should be noted that compositions that do not produce free-standing gels but appear to be predominantly worms by TEM are classified as mixed phases. These worms are rather polydisperse in terms of their length, but have well-defined widths that are close to the mean diameter of the spherical nanoparticles. This is because worm formation occurs via one-dimensional aggregation of monomer-swollen spheres during the BzMA polymerization (presumably because steric stabilization is less effective at the worm-ends due to their relatively high curvature and hence lower stabilizer chain density). Well-defined vesicles are obtained for PLMA<sub>17</sub>-PBzMA<sub>100-250</sub> and thicker vesicle membranes are produced when targeting higher DP values for the membrane-forming PBzMA block. Similar observations were made by Chambon et al. for

diblock copolymer vesicles generated during PISA syntheses conducted under RAFT aqueous dispersion polymerization conditions.<sup>22</sup>

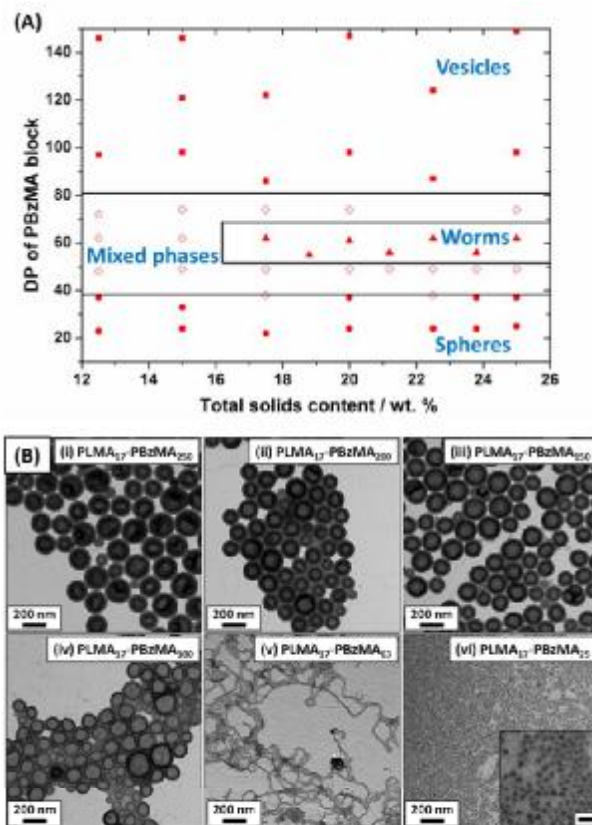


**Fig. 4** (A) Phase diagram constructed for PLMA<sub>17</sub>-PBzMA<sub>x</sub> diblock copolymer particles prepared by RAFT dispersion polymerization in *n*-heptane at 90 °C using T21s initiator. The PBzMA DP and the total solids content were systematically varied and the *post mortem* diblock copolymer morphologies obtained at high BzMA conversion (> 96 %) were determined by TEM. Filled squares (■), triangles (▲) and circles (●) correspond to pure phases of vesicles, worms and spheres respectively. Hollow diamonds (◇) correspond to worm/vesicle or sphere/worm mixed phases. (B) Representative TEM images obtained for PLMA<sub>17</sub>-PBzMA<sub>x</sub> nanoparticles synthesized by RAFT dispersion polymerization of BzMA in *n*-heptane at 90 °C and 20 wt. % solids (entries 25-28, 30 and 33 in Table S2). The targeted diblock compositions are indicated on each image. The inset in image (vi) shows a magnified area of the sample and the scale bar corresponds to 50 nm.

Overall, the phase diagram shown in Figure 4A indicates that the final diblock copolymer morphology is mainly dictated by the DP of the core-forming block, since only a rather weak concentration dependence is observed (mainly for the worm phase). Similar phase diagrams have been recently reported for other RAFT dispersion polymerization formulations.<sup>18, 19, 25, 26</sup>

It is perhaps noteworthy that highly asymmetric diblock copolymer compositions were also a pre-requisite in order to access worm and vesicle phase space for a particular RAFT aqueous dispersion polymerization formulation.<sup>19</sup> In this earlier study, the macro-CTA had a mean DP of 25 and was based on 2-(methacryloyloxy)ethyl phosphorylcholine (MPC), which has a comparable molar mass to that of LMA. In contrast, worm and

vesicular morphologies can be readily achieved via RAFT alcoholic dispersion polymerization formulations using much longer poly(methacrylic acid)-based CTAs (e.g. DP = 71).<sup>25</sup> Presumably, this is due to the significantly lower molar mass of the methacrylic acid repeat unit (86 g mol<sup>-1</sup>) compared to that of MPC (295 g mol<sup>-1</sup>) or LMA (254 g mol<sup>-1</sup>). Thus it seems that the overall *volume fraction* occupied by the stabilizer chains is a more important parameter than their mean DP in dictating the copolymer morphology formed in these PISA syntheses. This observation is consistent with previous findings by Discher and co-workers for diblock copolymer morphologies prepared by post-polymerization processing<sup>46</sup> and is closely related to the molecular packing model first proposed by Israelachvili<sup>47</sup> for classical surfactants, and later extended to block copolymers by Antonietti and Förster.<sup>48</sup>

From the above discussion, diblock copolymers such as PLMA<sub>38</sub>-PBzMA<sub>900</sub> most likely suffer a high degree of molecular frustration in their spherical form (see Figure 3). In principle, such highly asymmetric chains should prefer to form vesicles based on a simple molecular packing argument.<sup>18, 49</sup> For such kinetically trapped nanoparticles, we suggest that the diblock copolymer morphology cannot evolve beyond spheres because the mean DP of the PLMA block is sufficiently long to ensure effective steric stabilization, and hence prevent one-dimensional fusion of spheres to form worms, which is a key intermediate required for vesicle formation.<sup>20, 50</sup> Presumably, this is also the reason why Charleux et al. were only able to access spherical nanoparticles with their all-acrylic RAFT PISA formulation,<sup>38</sup> since the mean DP of their poly(2-ethylhexyl acrylate)-based macro-CTAs always exceeded 50.

Finally, we have recently extended this work to include the direct synthesis of all-methacrylic diblock copolymer nanoparticles with spherical, worm-like or vesicular morphologies in a range of non-polar solvents, such as *n*-dodecane, a C<sub>12</sub>-C<sub>15</sub> mineral oil and a low viscosity poly(α-olefin) oil. Although beyond the scope of the current study, these results illustrate the generic applicability of this PISA formulation and augur well for the potential use of such nanoparticles as boundary lubricants for engine oils (since acrylic copolymers are simply too susceptible to hydrolytic degradation to be useful in this context).

## Conclusions

We report the first example of an efficient all-methacrylic RAFT dispersion polymerization formulation for non-polar solvents such as *n*-heptane. The versatility of this new formulation is demonstrated by comparing the behavior of several macro-CTAs as the stabilizer block. A relatively long poly(lauryl methacrylate) macro-CTA allows the formation of spherical nanoparticles of tunable diameter, as judged by DLS and TEM studies. In contrast, the judicious selection of a relatively short macro-CTA enables the formation of higher order block copolymer morphologies such as worms or vesicles. In the latter case pure phases can be reproducibly targeted once a detailed phase diagram has been elucidated, with the worm phase proving to be the most elusive. GPC analysis indicates that relatively high blocking efficiencies and reasonably low final polydispersities can be achieved, as expected for RAFT syntheses. Bearing in

mind the aqueous and alcoholic RAFT formulations previously reported in the literature, the present study confirms the universal applicability of the polymerization-induced self-assembly (PISA) approach for the production of well-defined diblock copolymer nanoparticles of controlled size and shape. Given that RAFT polymerization chemistry has already been commercialized for the production of polymeric engine oil additives, the diblock copolymer ‘nano-objects’ described herein are expected to offer considerable potential as novel boundary lubricants for next-generation engine oil formulations.<sup>40</sup> This evaluation will be reported elsewhere in due course.

## Notes and references

- <sup>70</sup> <sup>a</sup> Dainton Building, Department of Chemistry, The University of Sheffield, Brook Hill, Sheffield, South Yorkshire, S3 7HF, UK. E-mail: [L.a.fieldding@shef.ac.uk](mailto:L.a.fieldding@shef.ac.uk) or [s.p.armes@shef.ac.uk](mailto:s.p.armes@shef.ac.uk)
- <sup>75</sup> <sup>b</sup> Ingénierie et Architectures Macromoléculaires, Institut Charles Gerhardt - UMR(CNRS) 5253, Ecole Nationale Supérieure de Chimie de Montpellier, 8, Rue de l'Ecole Normale, 34296 Montpellier Cedex, France.
- <sup>75</sup> <sup>c</sup> CSIRO Materials Science and Engineering, Bayview Avenue, Clayton, Vic 3168, Australia.
- <sup>80</sup> <sup>d</sup> Système Moléculaires Organisés et Développement Durable, Laboratoire des IMRCP, UMR(CNRS) 5623, Université Paul Sabatier, 118 route de Narbonne, 31062 Toulouse Cedex 9, France.
- <sup>85</sup> <sup>e</sup> 1. Department of Applied Chemistry and Biotechnology, Graduate School of Engineering, University of Fukui, 3-9-1 Bunkyo, Fukui 910-8507, Japan. 2. Japan Science and Technology Agency, PRESTO, 4-1-8 Honcho Kawaguchi, Saitama 332-0012, Japan.
- <sup>85</sup> † Electronic Supplementary Information (ESI) available: [PLMA polymerization kinetics, assigned <sup>1</sup>H NMR spectra and a PBzMA conversion vs. time graph are shown in Figures S1, S2 and S3 respectively. Tables S1, S2, S3 and S4 show summary tables including monomer conversions, calculated degrees of polymerization, GPC molecular weights, morphologies and particle diameters for the various polymers discussed].
1. J. T. Sun, C. Y. Hong and C. Y. Pan, *Soft Matter*, 2012, **8**, 3753-3767.
2. B. Charleux, G. Delaittre, J. Rieger and F. D'Agosto, *Macromolecules*, 2012, **45**, 6753-6765.
3. M. J. Monteiro and M. F. Cunningham, *Macromolecules*, 2012, **45**, 4939-4957.
4. J. Chiefari, Y. K. Chong, F. Ercole, J. Krstina, J. Jeffery, T. P. T. Le, R. T. A. Mayadunne, G. F. Meijs, C. L. Moad, G. Moad, E. Rizzardo and S. H. Thang, *Macromolecules*, 1998, **31**, 5559-5562.
5. S. Perrier and P. Takolpuckdee, *Journal of Polymer Science Part A-Polymer Chemistry*, 2005, **43**, 5347-5393.
6. L. Barner, T. P. Davis, M. H. Stenzel and C. Barner-Kowollik, *Macromolecular Rapid Communications*, 2007, **28**, 539-559.
7. G. Moad, E. Rizzardo and S. H. Thang, *Accounts of Chemical Research*, 2008, **41**, 1133-1142.
8. G. Moad, E. Rizzardo and S. H. Thang, *Polymer*, 2008, **49**, 1079-1131.
9. Z. An, Q. Shi, W. Tang, C.-K. Tsung, C. J. Hawker and G. D. Stucky, *J. Am. Chem. Soc.*, 2007, **129**, 14493-14499.
10. J. Rieger, C. Grazon, B. Charleux, D. Alaimo and C. Jerome, *Journal of Polymer Science Part A-Polymer Chemistry*, 2009, **47**, 2373-2390.
11. C. Grazon, J. Rieger, N. Sanson and B. Charleux, *Soft Matter*, 2011, **7**, 3482-3490.
12. G. Liu, Q. Qiu, W. Shen and Z. An, *Macromolecules*, 2011, **44**, 5237-5245.

- 
13. W. Shen, Y. Chang, G. Liu, H. Wang, A. Cao and Z. An, *Macromolecules*, 2011, **44**, 2524-2530.
14. S. Boisse, J. Rieger, K. Belal, A. Di-Cicco, P. Beaunier, M.-H. Li and B. Charleux, *Chem. Commun.*, 2010, **46**, 1950-1952.
15. A. Blanazs, R. Verber, O. O. Mykhaylyk, A. J. Ryan, J. Z. Heath, C. W. I. Douglas and S. P. Armes, *J. Am. Chem. Soc.*, 2012, **134**, 9741-9748.
16. R. Verber, A. Blanazs and S. P. Armes, *Soft Matter*, 2012, **8**, 9915-9922.
17. Y. Li and S. P. Armes, *Angew. Chem., Int. Ed.*, 2010, **49**, 4042-4046.
18. A. Blanazs, A. J. Ryan and S. P. Armes, *Macromolecules*, 2012, **45**, 5099-5107.
19. S. Sugihara, A. Blanazs, S. P. Armes, A. J. Ryan and A. L. Lewis, *J. Am. Chem. Soc.*, 2011, **133**, 15707-15713.
20. A. Blanazs, J. Madsen, G. Battaglia, A. J. Ryan and S. P. Armes, *J. Am. Chem. Soc.*, 2011, **133**, 16581-16587.
21. M. Semsarilar, V. Ladmiral, A. Blanazs and S. P. Armes, *Langmuir*, 2012, **28**, 914-922.
22. P. Chambon, A. Blanazs, G. Battaglia and S. P. Armes, *Macromolecules*, 2012, **45**, 5081-5090.
23. P. Chambon, A. Blanazs, G. Battaglia and S. P. Armes, *Langmuir*, 2012, **28**, 1196-1205.
24. S. Sugihara, S. P. Armes, A. Blanazs and A. L. Lewis, *Soft Matter*, 2011, **7**, 10787-10793.
25. M. Semsarilar, E. R. Jones, A. Blanazs and S. P. Armes, *Adv. Mater.*, 2012, **24**, 3378-3382.
26. E. R. Jones, M. Semsarilar, A. Blanazs and S. P. Armes, *Macromolecules*, 2012, **45**, 5091-5098.
27. J. N. Liu, H. E. Duong, M. R. Whittaker, T. P. Davis and C. Boyer, *Macromolecular Rapid Communications*, 2012, **33**, 760-766.
28. K. L. Thompson, P. Chambon, R. Verber and S. P. Armes, *J. Am. Chem. Soc.*, 2012.
29. W.-M. Wan, X.-L. Sun and C.-Y. Pan, *Macromolecular Rapid Communications*, 2010, **31**, 399-404.
30. W.-M. Wan and C.-Y. Pan, *Polym. Chem.*, 2010, **1**, 1475-1484.
31. C.-Q. Huang and C.-Y. Pan, *Polymer*, 2010, **51**, 5115-5121.
32. W.-D. He, X.-L. Sun, W.-M. Wan and C.-Y. Pan, *Macromolecules*, 2011, **44**, 3358-3365.
33. W. Cai, W. Wan, C. Hong, C. Huang and C. Pan, *Soft Matter*, 2010, **6**, 5554-5561.
34. C.-Q. Huang, Y. Wang, C.-Y. Hong and C.-Y. Pan, *Macromolecular Rapid Communications*, 2011, **32**, 1174-1179.
35. X. Zhang, J. Rieger and B. Charleux, *Polym. Chem.*, 2012, **3**, 1502-1509.
36. X. W. Zhang, S. Boisse, C. Bui, P. A. Albouy, A. Brulet, M. H. Li, J. Rieger and B. Charleux, *Soft Matter*, 2012, **8**, 1130-1141.
37. W. Ji, J. Yan, E. Chen, Z. Li and D. Liang, *Macromolecules*, 2008, **41**, 4914-4919.
38. L. Houillot, C. Bui, M. Save, B. Charleux, C. Farcet, C. Moire, J. A. Raust and I. Rodriguez, *Macromolecules*, 2007, **40**, 6500-6509.
39. M. Dan, F. Huo, X. Zhang, X. Wang and W. Zhang, *Journal of Polymer Science Part A: Polymer Chemistry*, 2013, **51**, 1573-1584.
40. R. Zheng, G. Liu, M. Devlin, K. Hux and T.-C. Jao, *Tribology Transactions*, 2010, **53**, 97-107.
41. A. B. Lowe and C. L. McCormick, *Prog. Polym. Sci.*, 2007, **32**, 283-351.
42. G. Moad, E. Rizzardo and S. H. Thang, *Australian Journal of Chemistry*, 2005, **58**, 379-410.
43. J. S. Trent, *Macromolecules*, 1984, **17**, 2930-2931.
44. A. D. Jenkins, D. Maxfield, C. G. Dossantos, D. R. M. Walton, J. Stejskal and P. Kratochvil, *Makromolekulare Chemie-Rapid Communications*, 1992, **13**, 61-63.
45. M. A. Awan, V. L. Dimonie and M. S. El-Aasser, *Journal of Polymer Science Part A-Polymer Chemistry*, 1996, **34**, 2633-2649.
46. D. E. Discher and A. Eisenberg, *Science*, 2002, **297**, 967-973.
47. J. N. Israelachvili, D. J. Mitchell and B. W. Ninham, *Journal of the Chemical Society, Faraday Transactions 2: Molecular and Chemical Physics*, 1976, **72**, 1525-1568.
48. M. Antonietti and S. Förster, *Adv. Mater.*, 2003, **15**, 1323-1333.
49. A. Blanazs, S. P. Armes and A. J. Ryan, *Macromolecular Rapid Communications*, 2009, **30**, 267-277.
50. D. Zehm, L. P. D. Ratcliffe and S. P. Armes, *Macromolecules*, 2012, **46**, 128-139.
-